SIMULATION OF TRAJECTORY CONTROL IN LIL

R. Chehab, Y. Thiery
Laboratoire de l'Accélérateur Linéaire (IN2P3)
Université de Paris-Sud, 91405-ORSAY (France)

K. Hübner
CERN-1211 Geneva, Switzerland

SUMMARY

The beam displacement due to misalignment errors
of the quadrupoles in the FODO array of the 600 MeV LEP
Injector Linac (LIL) is simulated using 30 statistical-
ly independent sets. The effects of displacement and
inclination are compared. Taking into account the ran-
dom errors in the position measurements, a trajectory
correction scheme using small corrector dipoles is tried
out on this sample of 30 FODO arrays. It is shown that
about five correctors are required to reduce the peak
distortion to less than 1 mm at the position monitors.
The aperture margin is increased by a factor 10 on ave-
rage in the most critical places.

INTRODUCTION

Geometrical misalignments in a linac cause tra-
jectory perturbations of the beam. Since the relative
emittance of the positron beam of LIL (36 π cm mrad
at 8 MeV) is relatively big, an accurate steering to
avoid beam losses in the accelerating sections is re-
quired.

Trajectory perturbations are due to quadrupole
misalignments (displacements and rotation of the qua-
drupole axis) accelerating-section misalignments and
gradient errors. Analytical evaluations showed that the
lateral quadrupole displacement is the more critical
misalignment for the beam[1]. Tilt of the quadrupoles
around one of their transverse axes is the effect next
in importance. Since it is of much less importance, all
results given later refer to lateral displacement of
quadrupoles. The detailed results for all types of
misalignments are given elsewhere[2].

Thirty statistically independent sets of misali-
gned FODO quadrupoles are produced for each misalignment
type considered. The perturbed trajectories are calcu-
lated using TRANSPORT[3].

The trajectory perturbations of the beam are
detected and corrected by a system of beam position
monitors (BPM) and steering dipoles (SD). The correction
configuration is computed with MICADO[4] in each case and
the corrected trajectory is then simulated using again
TRANSPORT. The quality of the correction can then be
determined by inspection of the residual perturbation.

The FODO quadrupoles are on the accelerating
sections ; as the relative energy gain over a quadru-
pole length is not always negligible, acceleration in
the quadrupoles was taken into account. The FODO system
is made up of 17 periods with a phase advance of 80°
per period. The beam position monitors are located
between the accelerating sections. The phase advance
between two adjacent monitors decreases slowly from 240°
to 80°. Correcting dipoles are in the focusing quadru-
poles with a period length of twice the FODO period.
This is very close to the actual situation in LIL. All
the calculations were done for the horizontal (x) and
vertical (y) plane. Due to the FODO structure the planes
are slightly different and, therefore, also the results
which are also influenced by the statistical variations.

SIMULATION OF THE PERTURBED MACHINES

The following quadrupole misalignments are consi-
dered : lateral displacement, rotation around the trans-
verse axis at the entrance of the quadrupole as well as
around the axis at its center. Misalignments errors are
randomly generated with Gaussian distributions having
the following standard deviations :

- lateral displacement : $\sigma = 0.3$ mm
- transverse axis rotation : 0.5 mrad
- error in beam position monitors : $\sigma = 0.2$ mm

All these distributions are truncated at $\pm 3\sigma$.

For the three kinds of misalignments we have cal-
culated the following functions for each group of 30
independent sets.

Mean and standard deviation for the perturbed trajectory

$$\bar{x}_i = \frac{1}{N} \sum_j x_{ij}$$

$$\langle x_i \rangle = \sqrt{\frac{1}{N-1} \sum_j (x_{ij} - \bar{x}_i)^2}$$

$$\langle x_{io} \rangle = \sqrt{\frac{1}{N-1} \sum_j x_{ij}^2}$$

where j is the machine index (j = 1,...30) and i the
quadrupole index. The results for the x-plane are shown
on figure 1. It can be seen that the standard deviation
grows according to $n^{1/2}$ as predicted[5] where n is the
number of FODO periods. If the standard deviations for
the three types of misalignments are compared, a factor
4 is found between the effects of the lateral displace-
ment and the rotation if the rotation is around the axis
at the entrance of the quadrupole, and a factor of 40 if
that inclination is at the center of the quadrupole.
This is consistent with the effects calculated for a
single quadrupole.

Histogram of maximum deviations

Figure 2 presents the histogram of maximum trajec-
tory distortions.

Relative beam displacement

This can be described by the function :

$$\overline{R_{1i}} = \frac{\overline{\Delta x_{qi}}}{a_i - b_i}$$

where Δx_{qi} is the beam displacement in the quadrupole q_i
a_i and b_i are iris radius value and beam dimension at
quadrupole q_i. The functions R_{1i} and Δx_{qi} are averaged
over 30 machines. The function $\overline{R_{1i}}$ is given for the x-y
planes in figure 3. It can be seen that in the horizontal
plane $\overline{R_{1i}}$ exceeds unity at three places and therefore
beam losses will occur on average.

CORRECTION OF THE PERTURBED MACHINES

MICADO[4] selects a subset of correctors indicating their strength and predicts the residual trajectory distortions after correction at the monitors. The correctors values are then introduced into TRANSPORT in order to determine the trajectory in the rest of the machine. MICADO minimizes the norm of the residual trajectory,

$$\vec{r} = \vec{b} + A\vec{x}$$

where $\vec{b}$ is the beam position indicated by the BPM, $\vec{x}$ the vector representing the correcting deflections,

A the correction matrix defined by $\dfrac{\partial \chi_{pi}}{\partial \chi'_{cj}}$ (trajectory

distortion at i-th BPM due to a unit deflection at j-th corrector).

At the first stage, each corrector is tried individually and the program choses the corrector which gives minimum norm for $\vec{r}$. At the second stage, pairs of correctors containing the first one already chosen are tested and the combination of correctors giving the minimum norm is retained.

The number of subsets is increased until the peak to peak trajectory distortion falls below a preset value or when the maximum allowed number of correctors is used.

Corrector strength

The behaviour of the following functions versus number of correctors has been studied :
Maximum corrector strength :

$$\overline{|B\ell|} = \frac{1}{N} \sum_{j=1}^{N} |\widehat{B\ell}|_j$$

Correction standard deviation :

$$< \overline{|B\ell|} > = \frac{1}{N} \sum_{j=1}^{N} \sqrt{\frac{1}{n_c - 1} \sum_{i=1}^{n_c} |B\ell|_{ij}^2}$$

where n_c is the number of correctors.

These functions plotted on figure 4 show that the correction standard deviation weakly depends on the number of correctors ; the maximum value is an increasing function of them.

Virtually the same curves are obtained in the case the measurement error is neglected. It is obvious from these results that the nominal corrector strength of 20 Gm, which has been chosen for LIL, is sufficient.

Residual trajectory distortions at the monitors
Maximum distortion :

$$\widehat{|D_x|} = \frac{1}{N} \sum_{j=1}^{N} |\widehat{D_x}|_j$$

and standard deviation :

$$< \overline{|D_x|} > = \frac{1}{N} \sum_{j=1}^{N} \sqrt{\frac{1}{n_p - 1} \sum_{i=1}^{n_p} |D_x|_{ij}^2}$$

where n_p is the number of BPM, are presented on figure 5.

The residual trajectory distortions are monotonically decreasing with increasing number of correctors and the standard deviation asymptotically reaches a value close to the BPM error standard deviation. For a maximum residual distortion of 1 mm, the number of correctors needed is about 5. The standard deviation of the residual trajectory does not exceed 0.8 mm for 3 correctors used.

Frequency of utilization of the correctors

The histogram on figure 6 gives the most requested correctors and a scatterplot (figure 7) presents the correlation between first and second correctors. It can be seen that the first and seventh correctors are often used together or with other correctors.

Relative beam displacement

The function $\overline{R_{1i}}$ has been computed with the corrector settings given by MICADO (figure 8). Comparison with figure 3 indicates that the relative beam displacement is much smaller on average after correction. Hence, the aperture margin is substantially increased and no more losses are to be expected.

An example of corrected trajectory

An example of the corrected trajectories in the x-plane is shown on figure 9 in a 3-corrector scheme. The first corrector strongly lowers the trajectory distortion, the subsequent correctors have a less drastic effect.

CONCLUSIONS

The simulations show clearly that the random quadrupole displacement has the strongest effect on the trajectory displacement in LIL. It could severely reduce the beam transmission through the linac if no correctors were used. The simulation show further that enough correctors are available to reduce the beam displacement to an acceptable value. It is likely that a subset of 4 to 5 correctors is sufficient. However, the members of the subset cannot yet be determined. The nominal corrector strength of 20 Gm is adequate. The on-line trajectory correction will use the same procedure as tested by the simulations and will be embedded in the on-line modelling facilities of the CERN PS control system.

The authors are indebted to Y. Marti from LEP division and G. Le Meur from LAL for helpful discussions.

REFERENCES

[1] R. Chehab. Internal note LAL/PI 83-28/T, Laboratoire de l'Accélérateur Linéaire, Orsay (France)

[2] R. Chehab, K. Hübner, Y. Thiery. Internal note PS/LPI/note 86-12 (CERN) and LAL PI 86-7/T (LAL)

[3] K.L. Brown and al. Transport CERN 80-04, March 1980

[4] B. Autin, Y. Marti. CERN ISR-MA/73-17

[5] R. Helm in the two mile accelerator. W.A. Benjamin Inc. 1968
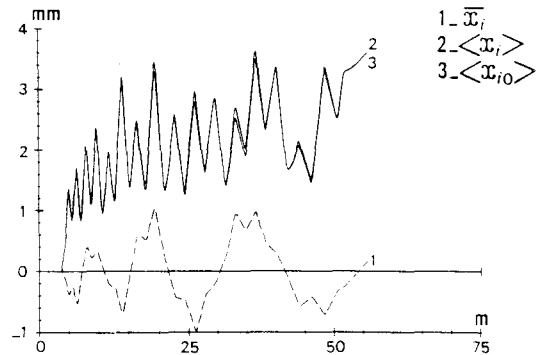
Fig. 1- Mean and standard deviation of the trajectories
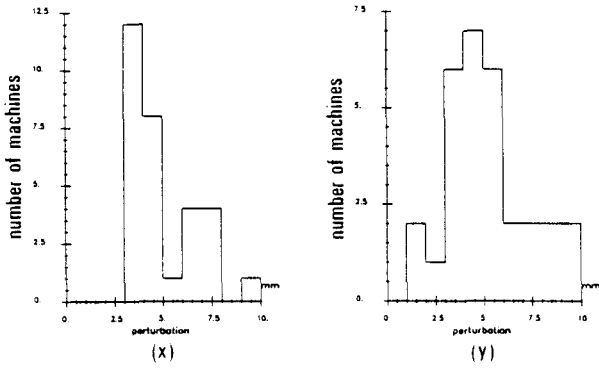
Fig. 2 - Histogram of maximum deviations
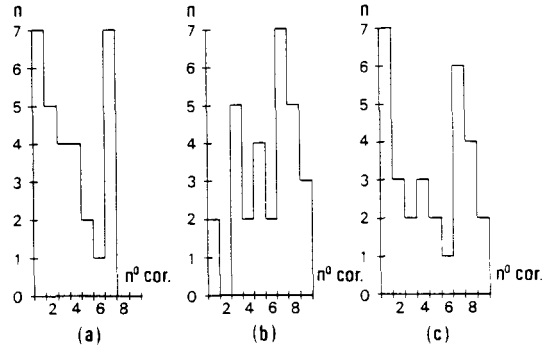
Fig. 6 - Histogram of the most requested correctors as 1st (a) - 2d (b) and 3d (c)
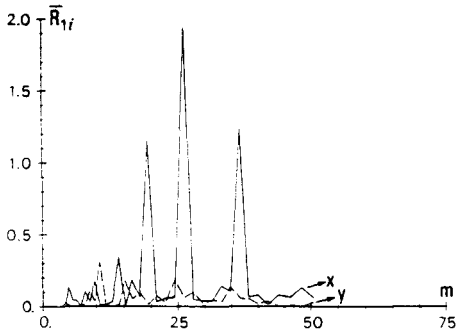
Fig. 3 - Relative beam displacement
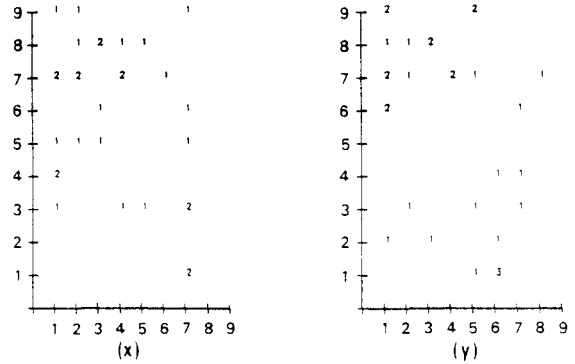
Fig. 7 - Scatterplot
Second corrector versus first corrector
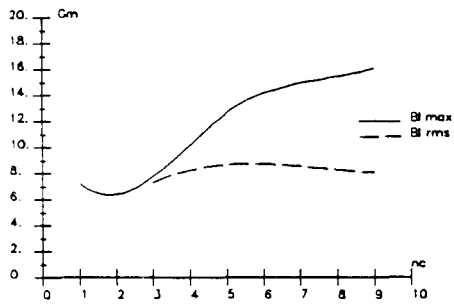
Fig. 4 - Corrector strength variation versus the number of correctors
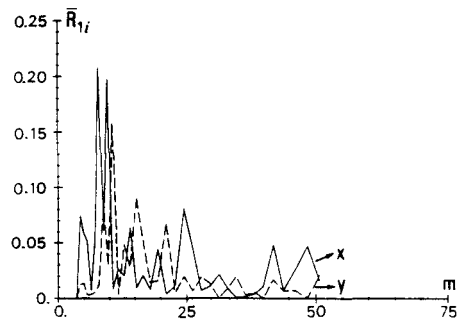
Fig. 8 - Relative beam displacement after correction
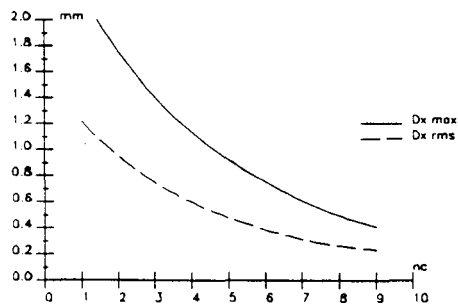
Fig. 5 - Residual trajectory in the monitors
n_c - number of correctors
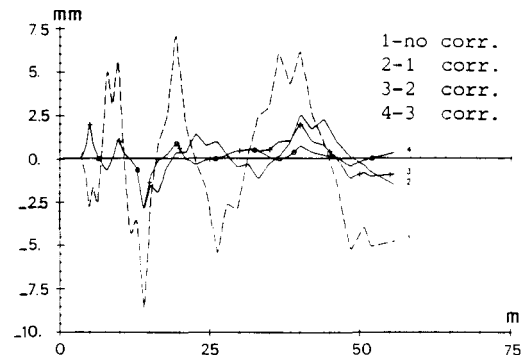
Fig. 9 - Example of corrected trajectory
Correctors used : 1-4-7